Renewable Energy 222 (2024) 119906

Contents lists available at ScienceDirect

Renewable Energy

journal homepage: www.elsevier.com/locate/renene

The impact of pumped hydro energy storage configurations on investment planning of hybrid systems with renewables

Gulin Yurter [a], Emre Nadar [a], Ayse Selin Kocaman [a,b,*]

[a] Department of Industrial Engineering, Bilkent University, Ankara, Turkey
[b] Energy Initiative, Massachusetts Institute of Technology, Cambridge, MA, USA

ARTICLE INFO

Keywords:
Pumped hydro energy storage
Renewable energy
Stochastic programming
Hybrid energy systems
Investment planning

ABSTRACT

The pumped hydro energy storage (PHES) systems can be installed in various configurations depending on the specific geographical and hydrological conditions. Closed-loop PHES systems are off-stream and have no natural inflow to the system. However, open-loop systems are on-stream and have natural inflows to the upper and/or lower reservoirs. In this study, we develop two-stage stochastic programming models for various PHES configurations to investigate how the choice of PHES configuration impacts the sizing decisions and costs of a hybrid system that includes a renewable power generator co-operated with PHES. Our numerical results show that using a PHES facility instead of a conventional hydropower system reduces the expected system cost and mismatched demand significantly. Open-loop PHES facilities perform better than closed-loop PHES and seawater-PHES facilities, dramatically lowering the need for fossil fuels in demand fulfillment. The most cost-efficient PHES configuration is when there is natural inflow to the upper reservoir. Using solar energy instead of wind as the renewable source significantly increases the requirement for larger upper reservoirs in on-stream open-loop PHES facilities, while reducing the expected system cost for all configurations.

1. Introduction

In recent years, renewable energy sources have received significant attention so as to reduce reliance on fossil fuels and mitigate their negative environmental impacts. Nearly two-thirds of the global power capacity additions are for wind and solar [1]. However, given the intermittent nature of these sources, it is necessary to support them with efficient and flexible storage systems to enhance their reliability. One such solution is pumped hydro energy storage (PHES), which stands out as one of the most widely adopted large-scale storage technologies to address the intermittency challenge of renewable sources [2]. PHES systems pump water to an elevated reservoir to store any available excess energy. This stored energy can be retrieved by releasing water from the upper reservoir to a lower one. Thanks to its superior environmental and financial performance when compared to many other storage technologies, PHES has emerged as one of the most commercially viable storage options [3] and accounts for 96% of the global power storage capacity [1].

The global installed capacity of PHES systems has shown a rapid increase in the past decade and has reached 130 GW in 2021 [5]. Fig. 1 exhibits this trend from 2010 to 2021. The distribution of the rated PHES capacity across different regions of the world can be observed in Fig. 2. The rapid expansion of PHES capacity in recent years has been accompanied by a significant increase in regional disparities. According to the International Renewable Energy Agency (IRENA), Asia currently has the highest PHES capacity in the world with a rated power of 72 GW, followed by Europe and North America with capacities of 28 GW and 22 GW, respectively. Africa and the Middle East lag far behind with capacities of 3.2 GW and 1.5 GW, respectively [4]. IRENA also reports that China leads the world with a capacity of 36 GW, followed by Japan with a capacity of 22 GW [4]. In North America, the United States has a capacity of 22 GW, while Canada lags behind with a capacity of only 177 MW [4,6]. Although Canada is the world's fourth-largest hydropower generator with a capacity of 81 GW as of 2019, its PHES capacity is limited [5].

While conventional hydropower remains of great interest globally with a capacity of 1360 GW in 2021 [5], the PHES systems have been gaining importance due to their potential to reduce the use of nonrenewable resources and improve load-balancing and resource allocation [7]. The growth trend of PHES systems is expected to continue as this technology becomes more widely recognized as a valuable tool for energy storage and grid stabilization. The PHES systems are typically classified into two primary types based on geographical conditions and natural water availability: open-loop vs. closed-loop [8]. Open-loop PHES systems rely on natural water inflow to supply upper and/or

* Corresponding author at: Department of Industrial Engineering, Bilkent University, Ankara, Turkey.
E-mail addresses: selin.kocaman@bilkent.edu.tr, kocaman@mit.edu (A.S. Kocaman).

https://doi.org/10.1016/j.renene.2023.119906
Received 16 August 2023; Received in revised form 17 November 2023; Accepted 26 December 2023
Available online 29 December 2023
0960-1481/

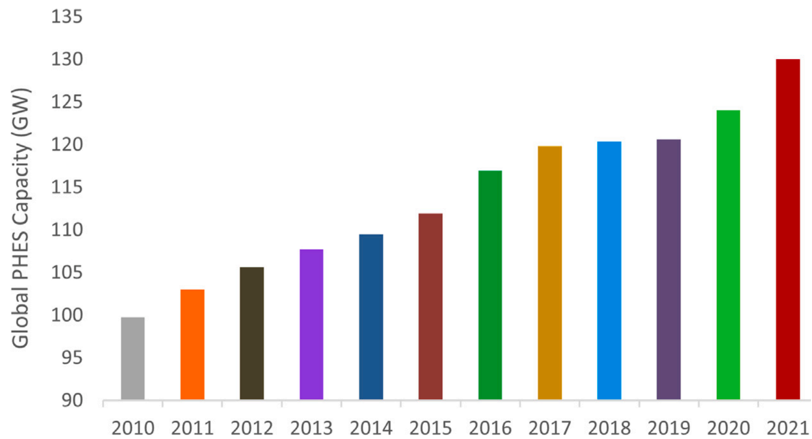

Fig. 1. Installed PHES capacity from 2010 to 2021 (GW) [4].

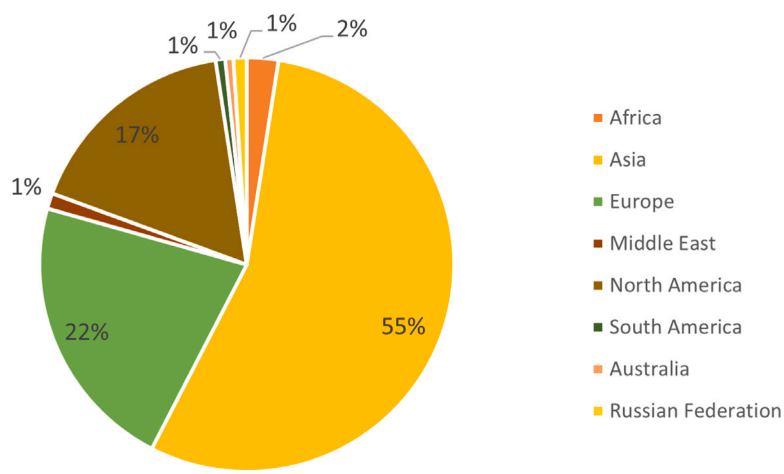

Fig. 2. Global PHES capacity distribution [4].

lower reservoirs, while closed-loop PHES operations are independent of the natural water inflow. In this study, we develop two-stage stochastic programming models for various PHES configurations to investigate how the choice of PHES configuration impacts the sizing decisions and costs of a hybrid system that includes a renewable source co-operated with PHES.

Considering the intermittencies of renewable resources and the uncertainties associated with them, it is a non-trivial task to optimize the sizing and operational decisions of hybrid energy systems with PHES. We refer the reader to Mahfoud et al. [9] and Toufani et al. [10] for comprehensive reviews of the PHES literature. In this literature, there are relatively fewer studies that model PHES systems via stochastic optimization frameworks, compared to deterministic approaches. The majority of stochastic optimization models focus only on the operational decisions of existing PHES systems. Two important examples of this category, which also motivated this study, are proposed by Toufani et al. [11,12]. Toufani et al. [11] examine the energy generation and storage problem for alternative PHES facilities (i.e., open-loop facilities with natural water inflow to upper and/or lower reservoirs and closed-loop facilities), formulating the problem as a stochastic dynamic program. Toufani et al. [12] study the energy generation and storage problem to evaluate the benefits of transforming conventional cascade hydropower stations into PHES systems, again modeling this operational problem as a stochastic dynamic program.

Optimizing the operations of hybrid energy systems with PHES is crucial for efficient control and management. However, it is also important to devise an optimal sizing plan under uncertainty to ensure a sufficient power supply without incurring excessive costs during the entire life cycle of the facility. In the literature dealing with the sizing problem under uncertainty, Zheng et al. [13] compare the dispatch strategies of various storage facilities, including a PHES facility. Brown et al. [14] address the question of how much pumped storage capacity to install for a PHES facility in a small island system. Reuter et al. [15] evaluate the economics of PHES systems with wind farms to stabilize profits from wind. Hemmati [16] proposes a renewable energy hub composed of wind–hydro–solar generation systems, supported by PHES and hydrogen storage systems, and optimizes system component capacities and operations to meet demand in autonomous buildings. Liu et al. [17] study the sizing problem for hydro-photovoltaic (PV)-pumped storage integrated generation system by taking into account the uncertainties in PV, spot price, and load. Elnozahy et al. [18] consider different hybrid storage options, including a PHES facility, by incorporating the weather uncertainty into a chance constraint. Abdalla et al. [19] study the sizing problem for wind-PHES systems by taking into account the wind and price uncertainties in their two-stage robust expansion planning model. Amusat et al. [20] solve a bi-criteria sizing problem to demonstrate the effects of intermittency and inter-year variability of renewable sources for several storage options, including a PHES facility. Within a hybrid system including PV panels and a costly diesel backup source, Kocaman and Modi [7] examine the value of a particular PHES configuration compared to a conventional hydropower station. Finally, Kocaman [21] presents two-stage stochastic programming models for mixed (a form of open-loop configuration) and pure (also known as seawater PHES configuration) PHES systems to study the sizing problem for hybrid energy systems.

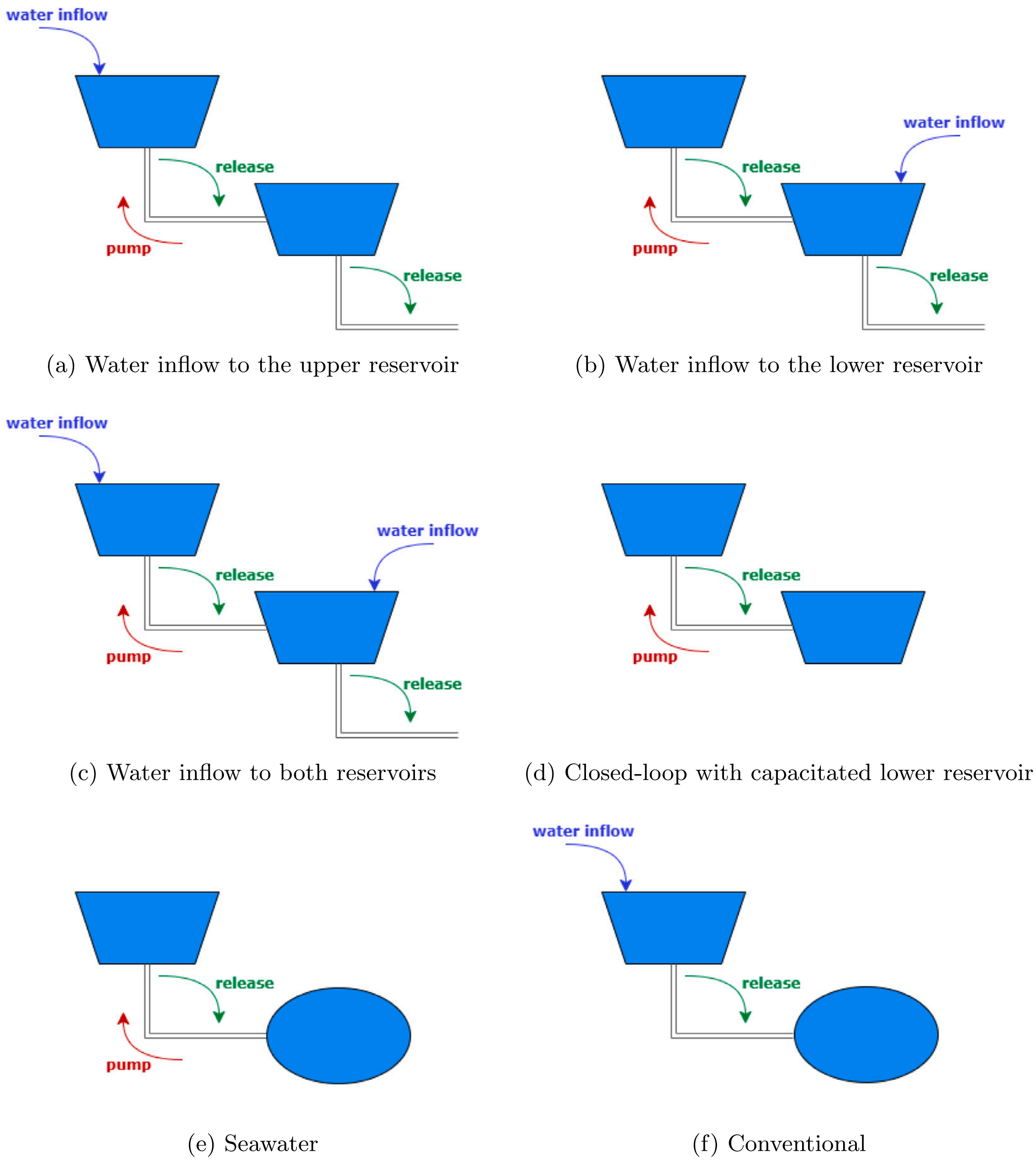

Fig. 3. (a)–(e) possible PHES configurations, (f) conventional hydropower station.

In this study, unlike Kocaman [21], we construct two-stage stochastic mixed-integer programming models for three different configurations of open-loop PHES systems: (i) the natural water flows only into the upper reservoir, (ii) it flows only into the lower reservoir, or (iii) it flows into both reservoirs. Furthermore, again unlike Kocaman [21], we extend these models to closed-loop, seawater and conventional hydropower systems (with no pumping capability). All these configurations are shown in Fig. 3. We study the sizing problem for these different configurations when they are integrated with a renewable source (solar or wind). The primary contributions of our study can be summarized as follows:

- Our study is the first to compare various open-loop PHES configurations (on-stream systems with natural inflow to upper and/or lower reservoirs) in terms of the optimal sizing decisions for system components. We also compare these configurations against closed-loop PHES facilities with capacitated lower reservoir, seawater-PHES facilities, and conventional hydropower systems. We perform all these comparisons in two different cases: when the hybrid energy system includes a solar farm or a wind farm.
- We develop two-stage stochastic mixed-integer programming models to optimize the sizing decisions for system components (e.g., the reservoir and generator capacities, solar panel area, and number of wind turbines) as well as the operational decisions (e.g., the amount of water to be pumped or released and the amount of energy to be curtailed).
- In our numerical experiments, we use real time-series data to take into account the streamflow uncertainty and measure the value of stochastic solution. With our numerical results, we offer new insights into the sizing decisions and costs of hybrid energy systems in different environments.

The rest of the paper is organized as follows: Section 2 formulates the two-stage stochastic programs for the sizing and operational planning problems of different PHES configurations. Section 3 presents the numerical results and their discussions. Section 4 presents the sensitivity results. Section 5 concludes by offering a summary.

2. Problem formulation

Our focus is on determining the optimal sizing of the hybrid system components (the PHES facility and the wind/solar farm) and the transmission line between the PHES facility and demand points. Fig. 4

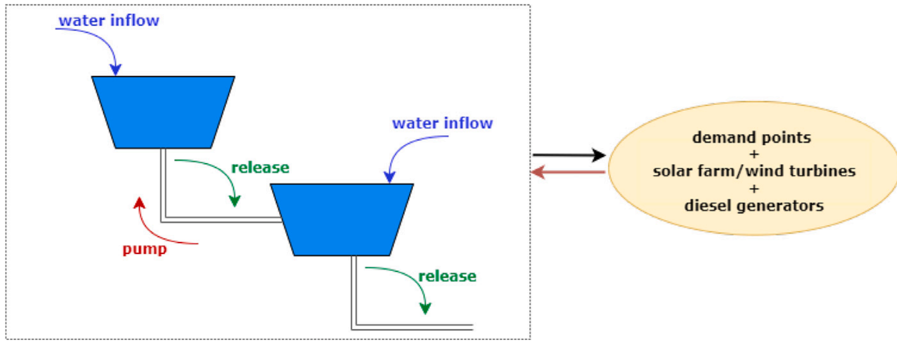

Fig. 4. A sample hybrid system with an open-loop PHES facility.

illustrates a hybrid energy system with a specific PHES configuration. In this system, the natural water flows into both reservoirs of the PHES facility and the hydropower generated can be transmitted to the demand points. Excess renewable energy generated in the demand points can be transmitted to the PHES facility to pump water from the lower reservoir to the upper reservoir to store it as gravitational potential energy. When the available renewable energy is not sufficient to meet the entire demand, we allow for a mismatch between supply and demand and a non-renewable resource like diesel can be used as a substitute. Like [7], we take the cost of diesel as the penalty for any mismatched demand, which is charged for each kWh of energy demand that hydropower or wind/solar power cannot meet.

2.1. Assumptions

In order to simplify the modeling of hydropower components, we make several commonly-used assumptions. Specifically, we assume that the water is always released from a constant height, the system efficiency is not affected by the amount of water pumped or released, and there is no loss of water in the PHES facility due to evaporation [21,22]. We consider a one-year planning horizon to capture the seasonal variability of renewable energy sources. We consider hourly energy generation and storage decisions to capture the intraday supply/demand variability. Since there is significant solar variability throughout the day, the use of hourly periods is needed [7]. Therefore, like [7], we employ a scenario-based model for the problem and utilize a one-year series with hourly periods.

2.2. Two-stage stochastic programming model

We construct a stochastic programming model consisting of two decision-making stages. The first-stage decisions x are made before the uncertainty is resolved, while the second-stage decisions y are made based on the resolved uncertainty. We can formulate the two-stage stochastic program in standard form as follows:

$$\min\ c^T x + \mathbb{E}_\omega[Q(x,\omega)] \tag{1}$$

$$\text{s.t. } Ax = b, \tag{2}$$

$$x \geq 0. \tag{3}$$

In the above formulation $Q(x,\omega)$ is the optimal solution to the second-stage problem with scenario ω. When there is a finite number of scenarios (realizations) and (d,h,T,W) is the data for the second-stage problem, we can find $Q(x,\omega)$ as follows [21,23]:

$$Q(x,\omega) = \min\left\{ d_\omega^T y_\omega | T_\omega x + W_\omega y_\omega = h_\omega,\ y_\omega \geq 0 \right\}. \tag{4}$$

The extended form of the scenario-based two-stage stochastic program can be written as follows:

$$\min\ c^T x + \sum_\omega p_\omega d_\omega^T y_\omega \tag{5}$$

$$\text{s.t. } Ax = b, \tag{6}$$

$$T_\omega x + W_\omega y_\omega = h_\omega \quad \forall\omega, \tag{7}$$

$$x \geq 0,\ y_\omega \geq 0 \quad \forall\omega. \tag{8}$$

For our problem, the first-stage decisions involve the sizing decisions for the system components, while the second-stage decisions involve the operational decisions that depend on the observed scenario. To address our research question, we construct two-stage stochastic programming models for each of the six different system configurations, including the conventional hydropower station in addition to five different PHES configurations. Indices, parameters, and decision variables of these models are given in Tables 1–3.

We present below our stochastic programming model for the hybrid system that includes the most general PHES configuration (i.e., an open-loop PHES system with water inflow to both upper and lower reservoirs) and a solar farm:

$$\begin{aligned}\text{minimize}\quad & d_h c_H \left(S_{U_{max}} + S_{L_{max}}\right) + d_h c_{PG}\left(PG_{U_{max}} + PG_{L_{max}}\right)\\ & + d_s c_S A + dist * d_t c_T T_{max} + \frac{\mu}{\Omega}\sum_{\omega=1}^{\Omega}\sum_{t=1}^{T} Z^{t\omega}\end{aligned} \tag{9}$$

Table 1
Indices for parameters and decision variables.

t	Time period 1,…,T, with a total of T periods
ω	Scenario 1,…, Ω, with a total of Ω scenarios

Table 2
Model parameters.

n	Length of each time period
d_h	Dimensionless annualization parameter for PHES systems
d_s	Dimensionless annualization parameter for solar power stations
d_w	Dimensionless annualization parameter for wind power stations
d_t	Dimensionless annualization parameter for transmission lines
l	Percentage power loss in transmission lines
g	Standard acceleration due to gravity
h_U	Height of the upper reservoir in the PHES system
h_L	Height of the lower reservoir in the PHES system
$dist$	Distance between the demand point and the PHES system
α	Efficiency of the PHES system in both generation and pump modes
γ	Efficiency of solar panels
c_H	Unit cost of reservoir capacity in hydropower station
c_{PG}	Unit cost of generator/pump capacity in hydropower station
c_S	Unit cost of solar panels
c_W	Unit cost of wind turbines
c_T	Unit cost of transmission line between the PHES system and the demand point
μ	Unit penalty for mismatched demand
p_ω	Weight of scenario ω, where $\sum_{\omega=1}^{\Omega} p_\omega = 1$
M	A large number

Table 3
Model variables.

Exogenous variables	
$SR^{t\omega}$	Solar radiation in period t in scenario ω
$WE^{t\omega}$	Energy generated from one wind turbine in period t in scenario ω
$ED^{t\omega}$	Energy demand in period t in scenario ω
$WU^{t\omega}$	Streamflow amount into the upper reservoir in period t in scenario ω
$WL^{t\omega}$	Streamflow amount into the lower reservoir in period t in scenario ω
Decision variables	
$S_{U_{max}}$	Upper reservoir capacity
$S_{L_{max}}$	Lower reservoir capacity
$PG_{U_{max}}$	Upper generator capacity
$PG_{L_{max}}$	Lower generator capacity
T_{max}	Transmission line capacity
A	Solar panel area
N	Number of wind turbines
$S_U^{t\omega}$	Water stored in the upper reservoir at the end of period t in scenario ω
$S_L^{t\omega}$	Water stored in the lower reservoir at the end of period t in scenario ω
$P^{t\omega}$	Water pumped to the upper reservoir in period t in scenario ω
$R_U^{t\omega}$	Water released from the upper reservoir in period t in scenario ω
$R_L^{t\omega}$	Water released from the lower reservoir in period t in scenario ω
$V^{t\omega}$	Solar energy directly used in the demand points in period t in scenario ω
$IP^{t\omega}$	Binary variable which is equal to 1 during pumping and equal to 0 during releasing in period t in scenario ω
$Z^{t\omega}$	Mismatched demand in period t in scenario ω
$L_U^{t\omega}$	Water spilled from the upper reservoir in period t in scenario ω
$L_L^{t\omega}$	Water spilled from the lower reservoir in period t in scenario ω
$C^{t\omega}$	Curtailed renewable energy in period t in scenario ω

subject to

$$S_U^{t\omega} = S_U^{t-1,\omega} + WU^{t\omega} + P^{t\omega} - R_U^{t\omega} - L_U^{t\omega} \quad \forall t > 1,\ \forall\omega, \tag{10}$$

$$S_L^{t\omega} = S_L^{t-1,\omega} + WL^{t\omega} - P^{t\omega} + R_U^{t\omega} - R_L^{t\omega} + L_U^{t\omega} - L_L^{t\omega} \quad \forall t > 1,\ \forall\omega, \tag{11}$$

$$S_U^{1\omega} = \frac{S_{U_{max}}}{2} + WU^{1\omega} + P^{1\omega} - R_U^{1\omega} - L_U^{1\omega} \quad \forall\omega, \tag{12}$$

$$S_L^{1\omega} = \frac{S_{L_{max}}}{2} + WL^{1\omega} - P^{1\omega} + R_U^{1\omega} - R_L^{1\omega} + L_U^{1\omega} - L_L^{1\omega} \quad \forall\omega, \tag{13}$$

$$S_U^{T\omega} = \frac{S_{U_{max}}}{2} \quad \forall\omega, \tag{14}$$

$$S_L^{T\omega} = \frac{S_{L_{max}}}{2} \quad \forall\omega, \tag{15}$$

$$S_U^{t\omega} \le S_{U_{max}} \quad \forall t,\ \forall\omega, \tag{16}$$

$$S_L^{t\omega} \le S_{L_{max}} \quad \forall t,\ \forall\omega, \tag{17}$$

$$\max\left\{ R_U^{t\omega} g h_U \alpha, \frac{P^{t\omega} g h_U}{\alpha} \right\} \le PG_{U_{max}} n \quad \forall t,\ \forall\omega, \tag{18}$$

$$R_L^{t\omega} g h_L \alpha \le PG_{L_{max}} n \quad \forall t,\ \forall\omega, \tag{19}$$

$$\max\left\{ \left(R_U^{t\omega} h_U + R_L^{t\omega} h_L\right) g\alpha, \frac{P^{t\omega} g h_U}{\alpha(1-l)} \right\} \le T_{max} n \quad \forall t,\ \forall\omega, \tag{20}$$

$$V^{t\omega} + \frac{P^{t\omega} g h_U}{\alpha(1-l)} + C^{t\omega} = A\gamma SR^{t\omega} \quad \forall t,\ \forall\omega, \tag{21}$$

$$ED^{t\omega} = Z^{t\omega} + V^{t\omega} + \left(R_U^{t\omega} h_U + R_L^{t\omega} h_L\right) g\alpha(1-l) \quad \forall t,\ \forall\omega, \tag{22}$$

$$P^{t\omega} \le IP^{t\omega} M \quad \forall t,\ \forall\omega, \tag{23}$$

$$R_U^{t\omega} \le \left(1 - IP^{t\omega}\right) M \quad \forall t,\ \forall\omega, \tag{24}$$

$$R_L^{t\omega} \le \left(1 - IP^{t\omega}\right) M \quad \forall t,\ \forall\omega, \tag{25}$$

$$IP^{t\omega} \in \{0,1\} \quad \forall t,\ \forall\omega, \tag{26}$$

$$\begin{aligned} &L_U^{t\omega}, L_L^{t\omega}, S_U^{t\omega}, S_L^{t\omega}, S_{U_{max}}, S_{L_{max}}, PG_{U_{max}}, PG_{L_{max}}, \\ &T_{max}, A, P^{t\omega}, R_U^{t\omega}, R_L^{t\omega}, V^{t\omega}, Z^{t\omega}, C^{t\omega} \ge 0 \quad \forall t,\ \forall\omega. \end{aligned} \tag{27}$$

The objective in Eq. (9) is to minimize the total system cost that includes the installation costs and the penalty costs for mismatched demand. For the installation costs, we multiply the sizes of all system components (upper and lower reservoirs, generators, solar panels, and transmission lines) by their unit installation costs and dimensionless annualization parameters. For the penalty costs, we calculate the total mismatched demand in each scenario, take the average over all scenarios, and multiply it by the unit penalty cost.

Eqs. (10) and (11) are the flow balance equations for the upper and lower reservoirs. We assume that both reservoirs are half-full at the beginning and end of the planning horizon. We incorporate this assumption into the flow balance equations with Eqs. (12) and (13) in the first period and with Eqs. (14) and (15) in the last period. Eqs. (16)–(20) set the capacity constraints for the upper and lower reservoirs, generators, and transmission lines, respectively. Eq. (21) ensures that the solar energy potential in any period is equal to the total amount of solar energy that is directly used to meet demand, utilized to pump water in the PHES facility, or curtailed in that period. Eq. (22) ensures that the demand is met by the hydro or solar energy generated, taking into account any mismatched demand. Together with Eq. (26), Eqs. (23), (24) and (25) are logical constraints that prohibit simultaneous pumping and releasing, affecting only the operational decisions.

2.3. Formulations for the alternative systems

2.3.1. Water inflow to the upper reservoir

When there is water inflow only to the upper reservoir, we update only the constraints that include the decision variable related to water inflow to the lower reservoir.

minimize (9)

subject to

$$S_U^{t\omega} = S_U^{t-1,\omega} + WU^{t\omega} + P^{t\omega} - R_U^{t\omega} - L_U^{t\omega} \quad \forall t > 1,\ \forall\omega,$$

$$S_L^{t\omega} = S_L^{t-1,\omega} - P^{t\omega} + R_U^{t\omega} - R_L^{t\omega} + L_U^{t\omega} - L_L^{t\omega} \quad \forall t > 1,\ \forall\omega,$$

$$S_U^{1\omega} = \frac{S_{U_{max}}}{2} + WU^{1\omega} + P^{1\omega} - R_U^{1\omega} - L_U^{1\omega} \quad \forall\omega,$$

$$S_L^{1\omega} = \frac{S_{L_{max}}}{2} - P^{1\omega} + R_U^{1\omega} - R_L^{1\omega} + L_U^{1\omega} - L_L^{1\omega} \quad \forall\omega,$$

(14)–(27).

2.3.2. Water inflow to the lower reservoir

minimize (9)
subject to

$$S_U^{t\omega} = S_U^{t-1,\omega} + P^{t\omega} - R_U^{t\omega} - L_U^{t\omega} \quad \forall t > 1,\ \forall \omega,$$

$$S_L^{t\omega} = S_L^{t-1,\omega} + WL^{t\omega} - P^{t\omega} + R_U^{t\omega} - R_L^{t\omega} + L_U^{t\omega} - L_L^{t\omega} \quad \forall t > 1,\ \forall \omega,$$

$$S_U^{1\omega} = \frac{S_{U_{max}}}{2} + P^{1\omega} - R_U^{1\omega} - L_U^{1\omega} \quad \forall \omega,$$

$$S_L^{1\omega} = \frac{S_{L_{max}}}{2} + WL^{1\omega} - P^{1\omega} + R_U^{1\omega} - R_L^{1\omega} + L_U^{1\omega} - L_L^{1\omega} \quad \forall \omega,$$

(14)–(27).

2.3.3. Closed-loop PHES facilities

Closed-loop PHES facilities have no natural water inflow. There is no water spillage in either reservoir and there is no power generation in the lower reservoir.

$$\text{minimize} \quad d_h c_H \left(S_{U_{max}} + S_{L_{max}}\right) + d_h c_{PG} PG_{U_{max}} + d_s c_S A + dist * d_t c_T T_{max} + \frac{\mu}{\Omega} \sum_{\omega=1}^{\Omega} \sum_{t=1}^{T} Z^{t\omega}$$

subject to

$$S_U^{t\omega} = S_U^{t-1,\omega} + P^{t\omega} - R_U^{t\omega} \quad \forall t > 1,\ \forall \omega,$$

$$S_L^{t\omega} = S_L^{t-1,\omega} - P^{t\omega} + R_U^{t\omega} \quad \forall t > 1,\ \forall \omega,$$

$$S_U^{1\omega} = \frac{S_{U_{max}}}{2} + P^{1\omega} - R_U^{1\omega} \quad \forall \omega,$$

$$S_L^{1\omega} = \frac{S_{L_{max}}}{2} - P^{1\omega} + R_U^{1\omega} \quad \forall \omega,$$

$$\max \left\{ R_U^{t\omega} hg\alpha, \frac{P^{t\omega} gh}{\alpha(1-l)} \right\} \le T_{max} n \quad \forall t,\ \forall \omega,$$

$$ED^{t\omega} = Z^{t\omega} + V^{t\omega} + R_U^{t\omega} hg\alpha\,(1-l) \quad \forall t,\ \forall \omega,$$

(14)–(18), (21), (23)–(27).

2.3.4. Seawater-PHES facilities

The seawater-PHES facilities are similar to the closed-loop PHES facilities, with the exception that the lower reservoir has no specified capacity and is regarded as a sea. We thus no longer include the decision variables $S_L^{t\omega}$ and $S_{L_{max}}$ in our model. We note that this configuration is equivalent to the pure PHES configuration in [21].

$$\text{minimize} \quad d_h c_H S_{U_{max}} + d_h c_{PG} PG_{U_{max}} + d_s c_S A + dist * d_t c_T T_{max} + \frac{\mu}{\Omega} \sum_{\omega=1}^{\Omega} \sum_{t=1}^{T} Z^{t\omega}$$

subject to

$$S_U^{t\omega} = S_U^{t-1,\omega} + P^{t\omega} - R_U^{t\omega} \quad \forall t > 1,\ \forall \omega,$$

$$S_U^{1\omega} = \frac{S_{U_{max}}}{2} + P^{1\omega} - R_U^{1\omega} \quad \forall \omega,$$

$$\max \left\{ R_U^{t\omega} hg\alpha, \frac{P^{t\omega} gh}{\alpha(1-l)} \right\} \le T_{max} n \quad \forall t,\ \forall \omega,$$

$$ED^{t\omega} = Z^{t\omega} + V^{t\omega} + R_U^{t\omega} hg\alpha\,(1-l) \quad \forall t,\ \forall \omega,$$

(14), (16), (18), (21), (23)–(27).

2.3.5. Conventional hydropower stations

The conventional hydropower stations have no pumping capability and no lower reservoir. We thus remove the decision variables $S_{L_{max}}$, $PG_{L_{max}}$, $S_L^{t\omega}$, $P^{t\omega}$, $R_L^{t\omega}$, and $L_L^{t\omega}$ from our model.

$$\text{minimize} \quad d_h c_H S_{U_{max}} + d_h c_{PG} PG_{U_{max}} + d_s c_S A + dist * d_t c_T T_{max} + \frac{\mu}{\Omega} \sum_{\omega=1}^{\Omega} \sum_{t=1}^{T} Z^{t\omega}$$

subject to

$$S_U^{t\omega} = S_U^{t-1\omega} + WU^{t\omega} - R_U^{t\omega} - L_U^{t\omega} \quad \forall t > 1,\ \forall \omega,$$

$$S_U^{1\omega} = \frac{S_{U_{max}}}{2} + WU^{1\omega} - R_U^{1\omega} - L_U^{1\omega} \quad \forall \omega,$$

$$R_U^{t\omega} gh\alpha \le PG_{U_{max}} n \quad \forall t,\ \forall \omega,$$

$$R_U^{t\omega} gh\alpha \le T_{max} n \quad \forall t,\ \forall \omega,$$

$$ED^{t\omega} = Z^{t\omega} + V^{t\omega} + R_U^{t\omega} gh\alpha\,(1-l) \quad \forall t,\ \forall \omega,$$

(14), (16), (21), (27).

2.4. Hybrid systems with wind farms

If the hybrid energy system includes a wind farm instead of a solar farm, Eq. (21) of our main model can be modified as follows:

$$V^{t\omega} + \frac{P^{t\omega} gh}{\alpha\,(1-l)} + C^{t\omega} = WE^{t\omega} N \quad \forall t,\ \forall \omega, \tag{28}$$

where the decision variable N is a nonnegative integer. For the other models, the corresponding constraints are changed to Eq. (28). In addition, the solar component of the objective function is replaced with the wind component. The objective function of our main model can thus be rewritten as follows:

$$\text{minimize} \quad d_h c_H \left(S_{U_{max}} + S_{L_{max}}\right) + d_h c_{PG} \left(PG_{U_{max}} + PG_{L_{max}}\right) + d_w c_W N + dist * d_t c_T T_{max} + \frac{\mu}{\Omega} \sum_{\omega=1}^{\Omega} \sum_{t=1}^{T} Z^{t\omega}.$$

3. Numerical experiments

We present a case study to examine the optimal sizing decisions of a hybrid energy system that can meet a peak demand of 1 GW in the Mediterranean region of Türkiye. This demand is met by solar/wind energy and hydro energy, which is generated by utilizing the water available from the Manavgat river [24]. The solar radiation and wind speed data is obtained for the same region from Homer Energy [25]. The excess solar/wind energy is stored in the PHES facilities, except for the conventional case with no storage option. We take into account the unpredictability of streamflow rate by incorporating the historical data of the previous 19 years into our models for the open-loop PHES facilities and conventional hydropower stations. We note that the closed-loop PHES facilities have no natural water inflow and thus involve no uncertainty.

The cost, efficiency, and lifetime parameters of the solar farm are obtained from [21] and are presented in Table 4. The unit cost of a wind turbine with 900 kW power capacity is assumed to be \$1.7M and its lifetime is assumed to be 20 years [26,27]. The distance between the hydroelectric system and the demand points is assumed to be 50 km. The DOcplex module of Python 3.9.7 was used to solve our models at a workplace with a 2.4 GHz Intel Xeon E5-2630 v3 CPU and 64 GB RAM.

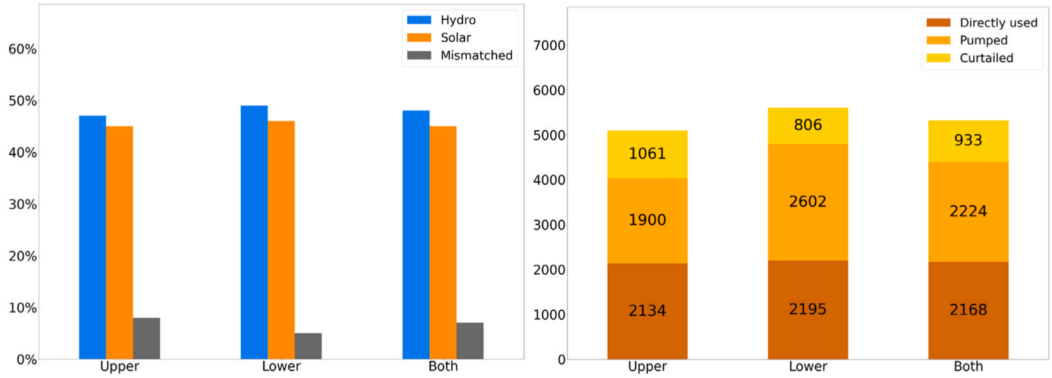

(a) Percentage contributions of resources (b) Solar energy utilization in GWh

Fig. 5. Comparison of systems with open-loop PHES and solar farms based on renewable energy contribution and solar energy utilization.

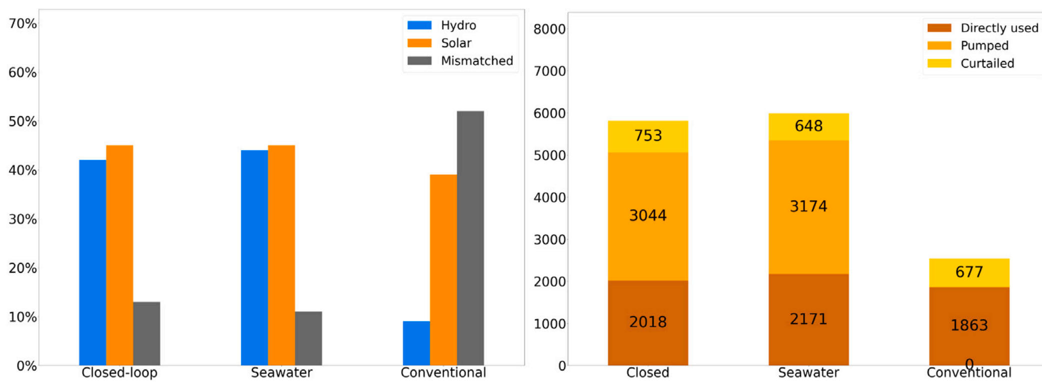

(a) Percentage contributions of resources (b) Solar energy utilization in GWh

Fig. 6. Comparison of closed-loop PHES systems, seawater-PHES systems, and conventional hydropower stations based on renewable energy contribution and solar energy utilization.

Table 4
Parameters values for numerical experiments.

Unit cost of reservoir	$3/m³
Unit cost of generator	$500/kW
Unit cost of solar panels	$200/m²
Unit cost of wind turbines	$1.7 M
Unit cost of diesel	$0.25/kWh
Cost of transmission line	$1.1 M/GW
One-sided efficiency of the hydroelectric system	88%
Efficiency of solar panels	12%
Discount factor	5%
Loss in transmission lines	5%
Height of the upper reservoir	100 m
Height of the lower reservoir	100 m
Lifetime of solar panels	30 years
Lifetime of the hydroelectric system	60 years
Lifetime of transmission lines	40 years
Lifetime of wind turbines	20 years

3.1. Analysis of systems with solar farms

We consider the systems with on-stream PHES separately from the systems with closed-loop PHES, seawater-PHES, and conventional hydropower stations. We present and discuss our results for these two groups in the following two subsections, respectively.

3.1.1. Systems with open-loop PHES

For our analysis, we assume that the amount of streamflow entering the system remains the same across different PHES configurations. When there is water inflow to both reservoirs, half of the streamflow feeds the upper reservoir and the other half feeds the lower reservoir. The optimal sizing decisions for the open-loop PHES systems are shown in Table 5.

The best open-loop system in terms of *expected* cost is the case when the water flows only into the upper reservoir. All component sizes in this case are smaller than those in the other cases. This is because the PHES reservoirs are used to store energy via water pumped, and the need for storage and pumping (and thus large reservoirs) is lower with water entering the system through the upper reservoir. We observe that the *expected* system costs decline as the component sizes decrease. However, the systems with smaller components benefit less from the renewable sources, leading to higher mismatched demand. We also observe an increase in curtailed solar energy as the component sizes decrease. This situation is another outcome of pumping less: the incoming solar energy tends to be curtailed if it is not used to pump water in the PHES facility.

The expected percentage contributions of renewable sources to meet the demand for open-loop PHES systems are presented in Fig. 5(a). The mismatched demand is below 8% for all open-loop PHES systems. When the water flows only into the lower reservoir, the mismatched demand is at its minimum, and there is slightly more reliance on hydro than the other two configurations. These results can be explained by the larger system components and increased pumping capability in this case. The hydro and solar contributions are 49% and 46%, respectively, in this case. When the water flows only into the upper reservoir, the hydro and solar contributions are 47% and 45%, respectively. When the water flows into both reservoirs, the hydro and solar contributions are 48% and 45%, respectively.

The expected utilized amounts of solar energy in pumping water and meeting demand directly, respectively, are shown in Fig. 5(b). The solar energy produced is lowest, with a total of 5096 GWh, when the

Table 5
Comparison of systems with open-loop PHES and solar farms.

Water inflow to	Upper reservoir		Lower reservoir		Both reservoirs	
Upper res. cap. (km^3)	0.146		0.365		0.229	
Lower res. cap. (km^3)	0.038		0.053		0.040	
Upper gen. cap. (GW)	1.404		1.556		1.468	
Lower gen. cap. (GW)	0.145		0.239		0.182	
Solar panel area (km^2)	23.293		25.610		24.343	
Transmission line cap. (GW)	1.478		1.638		1.545	
Expected solar utilization	GWh	%	GWh	%	GWh	%
Directly used solar	2134	42%	2195	39%	2168	41%
Pumped solar	1900	37%	2602	46%	2224	42%
Curtailed solar	1061	21%	806	14%	933	18%
Total solar produced	5096	100%	5603	100%	5326	100%
Expected energy generation	GWh	%	GWh	%	GWh	%
Upper hydro	1805	38%	1861	39%	1811	38%
Lower hydro	457	10%	502	11%	479	10%
Solar	2134	45%	2195	46%	2168	45%
Mismatched demand	380	8%	217	5%	317	7%
Total consumption	4775	100%	4775	100%	4775	100%
Expected system cost ($/kWh)	0.099		0.106		0.102	

Table 6
Comparison of closed-loop PHES systems, seawater-PHES systems, and conventional hydropower stations, all with solar farms.

System type	Closed-loop		Seawater		Conventional	
Upper res. cap. (km^3)	0.061		0.119		0.007	
Lower res. cap. (km^3)	0.061		-		-	
Upper gen. cap. (GW)	1.570		1.665		0.278	
Lower gen. cap. (GW)	-		-		-	
Solar panel area (km^2)	26.579		27.397		11.611	
Transmission line cap. (GW)	1.652		1.753		0.278	
Expected solar utilization	GWh	%	GWh	%	GWh	%
Directly used solar	2018	35%	2171	36%	1863	73%
Pumped solar	3044	52%	3174	53%	0	0%
Curtailed solar	753	13%	648	11%	677	27%
Total solar produced	5815	100%	5994	100%	2540	100%
Expected energy generation	GWh	%	GWh	%	GWh	%
Hydro	2135	42%	2084	44%	450	9%
Solar	2018	45%	2171	45%	1863	39%
Mismatched demand	622	13%	520	11%	2461	52%
Total consumption	4775	100%	4775	100%	4775	100%
Expected system cost ($/kWh)	0.119		0.116		0.162	

Table 7
Comparison of systems with open-loop PHES and wind farms.

Water inflow to	Upper reservoir		Lower reservoir		Both reservoirs	
Upper res. cap. (km^3)	0.065		0.075		0.070	
Lower res. cap. (km^3)	0.057		0.067		0.063	
Upper gen. cap. (GW)	0.960		1.128		1.057	
Lower gen. cap. (GW)	0.143		0.173		0.157	
Number of wind turbines	2569		2869		2740	
Transmission line cap. (GW)	1.010		1.188		1.112	
Expected wind utilization	GWh	%	GWh	%	GWh	%
Directly used wind	2379	59%	2543	57%	2489	58%
Pumped wind	740	18%	1195	27%	947	22%
Curtailed wind	898	22%	748	17%	848	20%
Total wind produced	4017	100%	4486	100%	4284	100%
Expected energy generation	GWh	%	GWh	%	GWh	%
Upper hydro	982	21%	844	18%	899	19%
Lower hydro	436	9%	455	9%	447	9%
Wind	2379	50%	2543	53%	2489	52%
Mismatched demand	987	21%	933	20%	939	20%
Total consumption	4775	100%	4775	100%	4775	100%
Expected system cost ($/kWh)	0.135		0.144		0.139	

water flows only into the upper reservoir. In this case, 46% of the solar energy generated is used to pump water, 41% is used to meet demand directly, and the remaining 13% is curtailed. The solar energy produced is highest, with a total of 5603 GWh, when the water flows only into the

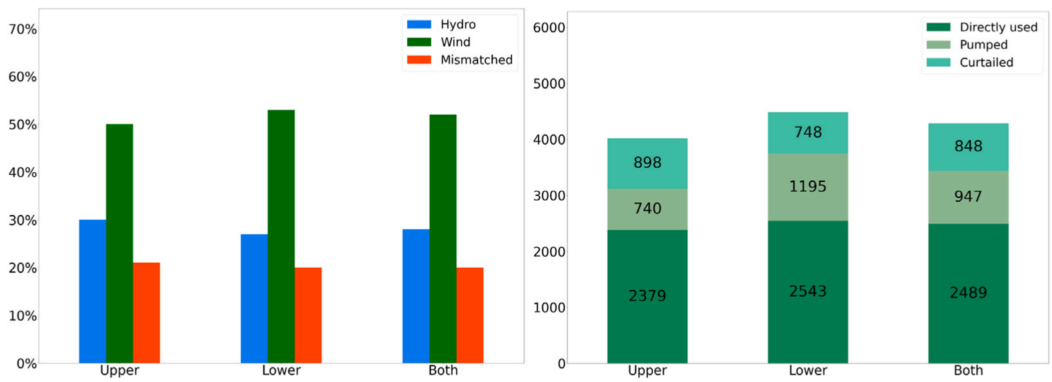

(a) Percentage contributions of resources (b) Wind energy utilization in GWh

Fig. 7. Comparison of systems with open-loop PHES and wind farms based on renewable energy contribution and wind energy utilization.

Table 8
Comparison of closed-loop PHES systems, seawater-PHES systems, and conventional hydropower stations, all with wind farms.

System type	Closed-loop		Seawater		Conventional	
Upper res. cap. (km^3)	0.105		0.142		0.008	
Lower res. cap. (km^3)	0.105		–		–	
Upper gen. cap. (GW)	1.435		1.449		0.156	
Lower gen. cap. (GW)	–		–		–	
Number of wind turbines	3395		3390		2040	
Transmission line cap. (GW)	1.510		1.526		0.156	
Expected wind utilization	GWh	%	GWh	%	GWh	%
Directly used wind	2491	47%	2601	49%	2225	70%
Pumped wind	2076	39%	2430	46%	0	0%
Curtailed wind	741	14%	270	5%	965	30%
Total wind produced	5308	100%	5300	100%	3190	100%
Expected energy generation	GWh	%	GWh	%	GWh	%
Hydro	1463	31%	1386	29%	221	5%
Wind	2491	52%	2601	55%	2252	47%
Mismatched demand	820	17%	787	17%	2328	49%
Total consumption	4775	100%	4775	100%	4775	100%
Expected system cost ($/kWh)	0.156		0.152		0.181	

Table 9
EVPI and VSS values for systems with open-loop PHES and solar farms.

Cost ($)/Water inflow	Upper	Lower	Both
RP	472,787,413	506,300,297	486,983,828
WS	468,418,476	503,617,172	483,311,016
EVPI	4,368,937	2,683,125	3,672,812
% EVPI	**0.92%**	**0.53%**	**0.75%**
EEV	474,482,019	516,157,139	491,208,620
VSS	1,694,606	9,856,842	4,224,791
% VSS	**0.36%**	**1.95%**	**0.87%**

Table 10
EVPI and VSS values for systems with open-loop PHES and wind farms.

Cost ($)/Water inflow	Upper	Lower	Both
RP	646,432,892	685,287,407	665,147,628
WS	645,406,104	684,022,405	662,753,772
EVPI	1,026,788	1,265,002	2,393,856
% EVPI	**0.16%**	**0.18%**	**0.36%**
EEV	651,941,889	686,329,963	668,805,385
VSS	5,508,998	1,042,557	3,657,756
% VSS	**0.85** %	**0.15%**	**0.55%**

lower reservoir. In this case, nearly 50% of the solar energy generated is used to pump water, 38% is used to meet demand directly, and 11% is curtailed. When the water flows into both reservoirs, 48% is used to pump water, 40% is used to meet demand directly, and 12% is curtailed.

3.1.2. Systems with closed-loop PHES, seawater-PHES, and conventional hydropower stations

The optimal sizing decisions for the closed-loop PHES systems, seawater-PHES systems, and conventional hydropower stations are shown in Table 6. We observe that the closed-loop PHES and seawater-PHES systems outperform the conventional hydropower stations in terms of expected cost. This is because the former two configurations have the energy storage capability while the conventional one does not. The closed-loop PHES and seawater-PHES systems also perform better in meeting demand from renewable resources, highlighting the importance of energy storage in renewable energy systems. The conventional hydropower station has a remarkably small upper reservoir capacity. This is because the system components incur high installation costs so that building a large upper reservoir is not beneficial if it is to be used purely as a generator with no storage option.

Fig. 6(a) shows that the expected percentage contributions of renewable sources to meet the demand are similar in the closed-loop PHES and seawater-PHES systems. The storage flexibility provided by the PHES configurations reduce the mismatched demand dramatically. While the mismatched demand is no larger than 13% for all of the PHES configurations, it is 52% for the conventional hydropower station. In our experiments the streamflow rate is the same in all system configurations. However, the hydro contribution is greater than 40% for all of the PHES configurations, but it is less than 10% for the conventional hydropower station. This result implies that the PHES systems utilize the available water inflow much more effectively than the conventional hydropower station. This result is expected since the solar energy

Table 11
Sensitivity analysis for open-loop PHES systems with solar farms.

Water inflow to	Diesel cost × 2			Base case			Diesel cost/2		
	Upper	Lower	Both	Upper	Lower	Both	Upper	Lower	Both
Upper. res. cap. (km^3)	0.499	0.542	0.517	0.146	0.365	0.229	0.026	0.027	0.025
Lower res. cap. (km^3)	0.063	0.071	0.066	0.038	0.053	0.040	0.017	0.023	0.020
Upper gen. cap. (GW)	1.557	1.608	1.587	1.404	1.556	1.468	0.609	0.844	0.718
Lower gen. cap. (GW)	0.139	0.205	0.171	0.145	0.239	0.182	0.165	0.203	0.186
Solar panel area (km^2)	25.632	27.145	26.298	23.293	25.610	24.343	13.466	16.211	14.726
Trans. line cap. (GW)	1.639	1.693	1.671	1.478	1.638	1.545	0.641	0.889	0.756
Water inflow to	Solar cost × 2			Base case			Solar cost/2		
	Upper	Lower	Both	Upper	Lower	Both	Upper	Lower	Both
Upper. res. cap. (km^3)	0.087	0.109	0.075	0.146	0.365	0.229	0.099	0.237	0.099
Lower res. cap. (km^3)	0.024	0.029	0.026	0.038	0.053	0.040	0.058	0.062	0.060
Upper gen. cap. (GW)	0.873	1.114	0.958	1.404	1.556	1.468	1.404	1.453	1.420
Lower gen. cap. (GW)	0.175	0.221	0.209	0.145	0.239	0.182	0.130	0.223	0.161
Solar panel area (km^2)	15.197	17.822	16.212	23.293	25.610	24.343	28.151	29.605	28.726
Trans. line cap. (GW)	0.919	1.172	1.009	1.478	1.638	1.545	1.478	1.530	1.495

Table 12
Sensitivity analysis for other systems with solar farms.

System type	Diesel cost × 2			Base case			Diesel cost/2		
	Closed	Seawater	Conv.	Closed	Seawater	Conv.	Closed	Seawater	Conv.
Upper. res. cap. (km^3)	0.084	1.191	0.019	0.061	0.119	0.007	0.029	0.034	0.005
Lower res. cap. (km^3)	0.084	–	–	0.061	–	–	0.029	–	–
Upper gen. cap. (GW)	1.688	1.574	0.332	1.570	1.665	0.278	1.030	1.031	0.220
Lower gen. cap. (GW)	–	–	–	–	–	–	–	–	–
Solar panel area (km^2)	31.684	29.703	16.628	26.579	27.397	11.611	18.347	18.238	8.336
Trans. line cap. (GW)	1.777	1.657	0.332	1.652	1.753	0.278	1.084	1.085	0.220
System type	Solar cost × 2			Base case			Solar cost/2		
	Closed	Seawater	Conv.	Closed	Seawater	Conv.	Closed	Seawater	Conv.
Upper. res. cap. (km^3)	0.051	0.063	0.006	0.061	0.119	0.007	0.062	0.093	0.008
Lower res. cap. (km^3)	0.051	–	–	0.061	–	–	0.062	–	–
Upper gen. cap. (GW)	1.387	1.408	0.266	1.570	1.665	0.278	1.523	1.548	0.297
Lower gen. cap. (GW)	–	–	–	–	–	–	–	–	–
Solar panel area (km^2)	20.694	20.836	8.380	26.579	27.397	11.611	32.342	32.157	16.587
Trans. line cap. (GW)	1.460	1.482	0.266	1.652	1.753	0.278	1.603	1.629	0.297

cannot be stored in the conventional hydropower station. Fig. 6(b) shows that the amount of solar energy produced in the conventional case is less than half of that in the other two configurations.

The open-loop PHES configurations have lower expected costs than the other PHES configurations. The upper reservoir capacities of open-loop configurations are much higher than those of the other configurations. Although the seawater-PHES system has no lower reservoir and thus has a distinct advantage in terms of installation costs, its upper reservoir capacity is less than that of the open-loop PHES systems. The closed-loop PHES and seawater-PHES systems (with no lower generator) have slightly higher upper generator capacities than the open-loop PHES systems. Since the closed-loop PHES and seawater-PHES systems generate less energy than the open-loop PHES systems, they require installation of wider solar panel areas, inducing larger amounts of solar energy produced. While the amounts of solar energy used to meet demand directly are not very different, the closed-loop PHES and seawater-PHES systems pump more water than the other systems. Although the seawater-PHES system has an access to unlimited amount of water, it has a slightly lower expected cost than the closed-loop PHES system and the amount of water pumped in the seawater-PHES system is only slightly greater than in the closed-loop PHES system.

3.2. Analysis of systems with wind farms

We rerun our numerical experiments by replacing the solar component of our hybrid energy system with the wind component. We present our results in the following two subsections.

3.2.1. Systems with open-loop PHES

We again assume that the amount of streamflow entering the system remains the same across different PHES configurations. When there is water inflow to both reservoirs, half of the streamflow feeds the upper reservoir and the other half feeds the lower reservoir. The optimal sizing decisions for the open-loop PHES systems are shown in Table 7.

Similar to the systems with solar farms, the expected system cost and component sizes are lowest when the water flows only into the upper reservoir. However, the sizing decisions of different components are closer here than in the systems with solar farms. Fig. 7(a) shows that the wind farm is the major source of energy, followed by the hydropower station, in all three PHES configurations. Figs. 5(b) and 7(b) indicate that the amounts of wind energy used to meet demand directly here are larger than the amounts of solar energy used to meed demand directly in the case with solar farms. The amounts of wind energy used to pump water here are smaller than the amounts of solar energy used to pump water in the case with solar farms. These results can be explained by varying levels of availability of renewable resources during the day. While the wind can be available throughout the day, the solar is available only during the daytime. The solar energy should be stored during the daytime if it is to be utilized during the night. Since the solar energy is stored more, the reservoir capacities and the amounts of water pumped are larger in the case with solar farms.

3.2.2. Systems with closed-loop PHES, seawater-PHES, and conventional hydropower stations

The optimal sizing decisions for the closed-loop PHES systems, seawater-PHES systems, and conventional hydropower stations are shown in Table 8. Fig. 8(a) shows that the wind farm is again the major

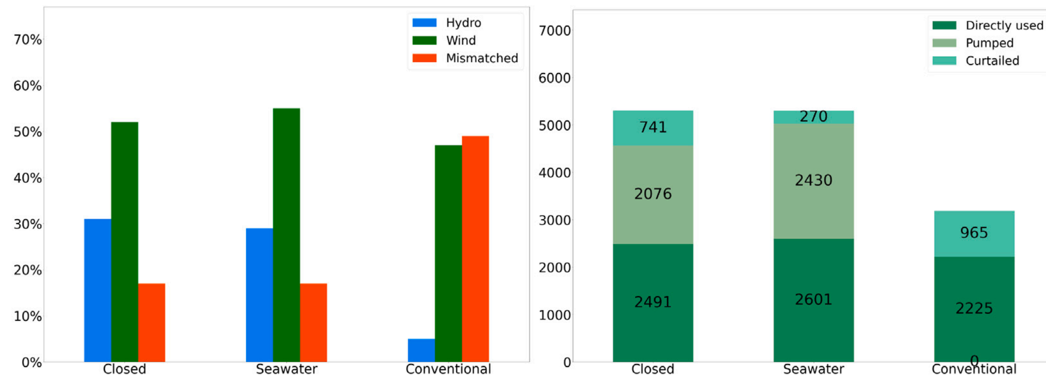

(a) Percentage contributions of resources (b) Wind energy utilization in GWh

Fig. 8. Comparison of closed-loop PHES systems, seawater-PHES systems, and conventional hydropower stations based on renewable energy contribution and wind energy utilization.

source of energy in all these systems. Fig. 6(b) and Fig. 8(b) indicate that the amounts of wind energy used to meet demand directly here are larger than the amounts of solar energy used to meed demand directly in the case with solar farms. The amounts of wind energy used to pump water here are smaller than the amounts of solar energy used to pump water in the case with solar farms. For the closed-loop PHES and seawater-PHES systems, the mismatched demand here is higher than in the case with solar farms. This is because the solar energy is stored more than the wind energy, and the stored renewable energy helps reduce the mismatched demand more effectively. Finally, the seawater-PHES systems experience very little curtailment of wind energy.

3.3. The impact of hydropower uncertainty

Two main indicators for assessing the importance of solving our two-stage stochastic programming models (for the open-loop PHES configurations) are the Expected Value of Perfect Information (EVPI) and the Value of Stochastic Solution (VSS). Our computations of EVPI and VSS are based on the methods described in [28]. We refer to the problem given in Section 2.2 by Eqs. (5)–(8) as the recourse problem. We compute EVPI by solving a deterministic problem for each scenario individually, averaging the optimal cost values of all these problems to obtain the *wait-and-see* solution (WS), and comparing it with the optimal cost of the recourse problem (RP). Specifically, let G_ω denote the optimal cost of the following deterministic problem for scenario ω:

$$\begin{aligned} \min\ & c^T x + d_\omega^T y_\omega \\ \text{s.t.}\ & Ax = b, \\ & T_\omega x + W_\omega y_\omega = h_\omega, \\ & x \geq 0,\ \ y_\omega \geq 0. \end{aligned}$$

Hence WS $= \frac{\sum_{\omega=1}^{\Omega} G_\omega}{\Omega}$ and EVPI $=$ RP $-$ WS. EVPI represents the maximum amount of money that one would be willing to pay to obtain perfect information about the future streamflow rates. For computation of VSS, we first calculate the scenario $\bar{\omega}$ by averaging all available scenarios in the recourse problem. We then solve the following deterministic problem for scenario $\bar{\omega}$:

$$\begin{aligned} \min\ & c^T x + d_{\bar{\omega}}^T y_{\bar{\omega}} \\ \text{s.t.}\ & Ax = b, \\ & T_{\bar{\omega}} x + W_{\bar{\omega}} y_{\bar{\omega}} = h_{\bar{\omega}}, \\ & x \geq 0,\ \ y_{\bar{\omega}} \geq 0. \end{aligned}$$

We refer to the solution of the above problem as the *expected value solution* and denote by $\bar{x}$ its first-stage decisions. We next implement these first-stage decisions into the recourse problem as follows:

$$\begin{aligned} \min\ & c^T \bar{x} + \sum_{\omega} p_\omega d_\omega^T y_\omega \\ \text{s.t.}\ & A\bar{x} = b, \\ & T_\omega \bar{x} + W_\omega y_\omega = h_\omega \quad \forall \omega, \\ & y_\omega \geq 0 \quad \forall \omega. \end{aligned}$$

The optimal cost of the above problem yields the expected result of taking the first-stage decisions of the expected value solution and the optimal second-stage decisions (conditional on the first-stage decisions). We obtain VSS by comparing this expected result (EEV) with the optimal cost of the recourse problem: VSS = EEV − RP. Tables 9 and 10 exhibit the EVPI and VSS values for the open-loop PHES systems with solar farms and wind farms, respectively. Tables 9 and 10 also show the EVPI and VSS percentages that are calculated as $\frac{EVPI}{RC} \times 100$ and $\frac{VSS}{RC} \times 100$, respectively.

We observe that the EVPI and VSS percentages are larger in the case with solar farms than in the case with wind farms in general. These results can be explained by the higher degree of intermittency of solar radiation and the resulting lower flexibility in handling uncertainty. An exception to this observation arises in the VSS percentage when the system has a solar farm and the water flows only into the upper reservoir. This result implies that the first-stage decisions (i.e., the sizing decisions) of the expected value solution are similar to the optimal first-stage decisions of the stochastic model, leading to a smaller VSS percentage in this specific case.

4. Sensitivity analysis

We performed sensitivity analysis by changing the unit cost of diesel (that we use as a proxy for the cost of backup source) and the unit installation costs of solar/wind farms. The results are shown in Tables 11–14. The "base case" columns of all these tables correspond to our results in Section 3. The upper panels of all these tables show how the optimal sizing decisions vary when we double the unit cost of diesel (μ) or halve it. The lower panels of Tables 11 and 12 show how the optimal sizing decisions vary when we double the unit installation cost of solar farm (c_S) or halve it. The lower panels of Tables 13 and 14 show how the optimal sizing decisions vary when we double the unit installation cost of wind farm (c_W) or halve it.

As expected, the optimal sizes of solar/wind farms grow as the diesel cost increases or as the installation costs decrease. For the systems with open-loop PHES and solar farms, the upper reservoir/generator capacity is more sensitive to changes in the diesel and solar installation costs, in comparison with the lower reservoir/generator capacity. The cost changes have a larger impact on the upper reservoir capacity of the seawater-PHES system than on those of the closed-loop PHES system and the conventional hydropower station. This result can be attributed to the larger upper reservoir of seawater-PHES system in general. For the systems with open-loop PHES and wind farms, the

Table 13
Sensitivity analysis for open-loop PHES systems with wind farms.

Water inflow to	Diesel cost × 2			Base case			Diesel cost/2		
	Upper	Lower	Both	Upper	Lower	Both	Upper	Lower	Both
Upper. res. cap. (km^3)	1.016	0.931	0.987	0.065	0.075	0.070	0.021	0.014	0.017
Lower res. cap. (km^3)	0.110	0.130	0.122	0.057	0.067	0.063	0.008	0.010	0.008
Upper gen. cap. (GW)	1.424	1.627	1.517	0.960	1.128	1.057	0.274	0.319	0.255
Lower gen. cap. (GW)	0.164	0.180	0.169	0.143	0.173	0.157	0.176	0.206	0.189
# wind turbines	3490	3854	3654	2569	2869	2740	1101	1283	1177
Trans. line cap. (GW)	1.499	1.712	1.596	1.010	1.188	1.112	0.450	0.363	0.444
Water inflow to	Wind cost × 2			Base case			Wind cost/2		
	Upper	Lower	Both	Upper	Lower	Both	Upper	Lower	Both
Upper. res. cap. (km^3)	0.059	0.040	0.041	0.065	0.075	0.070	0.071	0.085	0.076
Lower res. cap. (km^3)	0.015	0.023	0.019	0.057	0.067	0.063	0.065	0.075	0.069
Upper gen. cap. (GW)	0.379	0.615	0.490	0.960	1.128	1.057	1.294	1.467	1.375
Lower gen. cap. (GW)	0.175	0.232	0.203	0.143	0.173	0.157	0.102	0.112	0.108
# wind tubines	1200	1551	1369	2569	2869	2740	4048	4425	4236
Trans. line cap. (GW)	0.554	0.648	0.557	1.010	1.188	1.112	1.363	1.544	1.447

Table 14
Sensitivity analysis for other systems with wind farms.

System type	Diesel cost × 2			Base case			Diesel cost/2		
	Closed	Sewater	Conv.	Closed	Sewater	Conv.	Closed	Sewater	Conv.
Upper. res. cap. (km^3)	0.149	0.224	0.025	0.105	0.142	0.008	0.009	0.015	0.002
Lower res. cap. (km^3)	0.149	–	–	0.105	–	–	0.009	–	–
Upper gen. cap. (GW)	2.230	2.169	0.230	1.435	1.449	0.156	0.271	0.391	0.105
Lower gen. cap. (GW)	–	–	–	–	–	–	–	–	–
# wind turbines	4845	4707	3665	3395	3390	2040	1266	1408	944
Trans. line cap. (GW)	2.347	2.283	0.230	1.010	1.526	0.156	0.285	0.411	0.105
System type	Wind cost × 2			Base case			Wind cost/2		
	Closed	Sewater	Conv.	Closed	Sewater	Conv.	Closed	Sewater	Conv.
Upper. res. cap. (km^3)	0.029	0.055	0.004	0.105	0.142	0.008	0.096	0.145	0.013
Lower res. cap. (km^3)	0.029	–	–	0.105	–	–	0.096	–	–
Upper gen. cap. (GW)	0.722	0.883	0.138	1.435	1.449	0.156	1.546	1.773	0.183
Lower gen. cap. (GW)	–	–	–	–	–	–	–	–	–
# wind turbines	1714	1907	948	3395	3390	2040	4708	4975	3653
Trans. line cap. (GW)	0.760	0.929	0.138	1.010	1.526	0.156	1.628	1.867	0.183

upper reservoir/generator capacity is more sensitive to changes in the diesel cost (but not in the wind installation cost), in comparison with the lower reservoir/generator capacity. The cost changes again have a greater impact on the upper reservoir capacity of the seawater-PHES system than on those of the closed-loop PHES system and the conventional hydropower station.

5. Conclusion

In this study, we present two-stage stochastic mixed-integer programming models for various PHES configurations and investigate how the choice of PHES configuration impacts the sizing decisions of hybrid energy systems with solar/wind farms. We conduct numerical experiments by utilizing the real historical data of streamflow rates to generate the scenarios of our stochastic programming models. Our results show that the PHES systems can significantly reduce the need for fossil fuels in both cases of solar and wind farms. The open-loop PHES configurations perform better than the other PHES configurations in terms of expected system costs. For the open-loop PHES systems, the system cost is lowest when the water flows only into the upper reservoir.

This study and its results may lead to many different studies in the future. In order to reflect the real-life situations better, the uncertainties not only in the streamflow rate but also in the other renewable sources might be jointly incorporated into stochastic programming models. Such an extension will likely require a larger number of scenarios, leading to large-scale problems that are computationally challenging. Such problems may be solved by developing and using decomposition-based solution techniques such as L-shaped method [24]. Future research may also consider jointly optimizing the sizing and operational decisions via multi-stage stochastic programming models. Lastly, future work may look into the environmental and social aspects of the sizing and operational decisions.

CRediT authorship contribution statement

Gulin Yurter: Conceptualization, Methodology, Formal analysis, Software, Investigation, Writing – review & editing, Writing – original draft. **Emre Nadar:** Conceptualization, Methodology, Formal analysis, Writing – review & editing, Writing – original draft, Supervision. **Ayse Selin Kocaman:** Conceptualization, Methodology, Formal analysis, Writing – review & editing, Writing – original draft, Supervision.

Declaration of competing interest

The authors declare that they have no known competing financial interests or personal relationships that could have appeared to influence the work reported in this paper.

References

[1] Andrew Blakers, Matthew Stocks, Bin Lu, Cheng Cheng, A review of pumped hydro energy storage, Prog. Energy 3 (2) (2021) 022003.
[2] Shafiqur Rehman, Luai M. Al-Hadhrami, Md. Mahbub Alam, Pumped hydro energy storage system: A technological review, Renew. Sustain. Energy Rev. 44 (2015) 586–598.
[3] A.G. Olabi, C. Onumaegbu, Tabbi Wilberforce, Mohamad Ramadan, Mohammad Ali Abdelkareem, Abdul Hai Al-Alami, Critical review of energy storage systems, Energy 214 (2021) 118987.

[4] Renewable Capacity Statistics 2022, Technical Report, International Renewable Energy Agency, 2022.
[5] 2022 Hydropower Status Report, Technical Report, International Hydropower Association, 2022.
[6] 2021 Pumped Storage Report, Technical Report, National Hydropower Association, 2021.
[7] Ayse Selin Kocaman, Vijay Modi, Value of pumped hydro storage in a hybrid energy generation and allocation system, Appl. Energy 205 (2017) 1202–1215.
[8] Julian David Hunt, Behnam Zakeri, Rafael Lopes, Paulo Sérgio Franco Barbosa, Andreas Nascimento, Nivalde José de Castro, Roberto Brandão, Paulo Smith Schneider, Yoshihide Wada, Existing and new arrangements of pumped-hydro storage plants, Renew. Sustain. Energy Rev. 129 (2020) 109914.
[9] Rabea Jamil Mahfoud, Nizar Faisal Alkayem, Yuquan Zhang, Yuan Zheng, Yonghui Sun, Hassan Haes Alhelou, Optimal operation of pumped hydro storage-based energy systems: A compendium of current challenges and future perspectives, Renew. Sustain. Energy Rev. 178 (2023) 113267.
[10] Parinaz Toufani, Ece Cigdem Karakoyun, Emre Nadar, Olav B. Fosso, Ayse Selin Kocaman, Optimization of pumped hydro energy storage systems under uncertainty: A review, J. Energy Storage 73 (2023) 109306.
[11] Parinaz Toufani, Emre Nadar, Ayse Selin Kocaman, Short-term assessment of pumped hydro energy storage configurations: Up, down, or closed? Renew. Energy 201 (2022) 1086–1095.
[12] Parinaz Toufani, Emre Nadar, Ayse Selin Kocaman, Operational benefit of transforming cascade hydropower stations into pumped hydro energy storage systems, J. Energy Storage 51 (2022) 104444.
[13] Menglian Zheng, Christoph J. Meinrenken, Klaus S. Lackner, Smart households: Dispatch strategies and economic analysis of distributed energy storage for residential peak shaving, Appl. Energy 147 (2015) 246–257.
[14] Paul D. Brown, J.A. PeÇas Lopes, Manuel A. Matos, Optimization of pumped storage capacity in an isolated power system with large renewable penetration, IEEE Trans. Power Syst. 23 (2) (2008) 523–531.
[15] Wolf Heinrich Reuter, Sabine Fuss, Jana Szolgayová, Michael Obersteiner, Investment in wind power & pumped storage in a real options model– A policy analysis, Renew. Sustain. Energy Rev. 16 (4) (2012) 2242–2248.
[16] Reza Hemmati, Stochastic energy investment in off-grid renewable energy hub for autonomous building, IET Renew. Power Gener. 13 (12) (2019) 2232–2239.
[17] Jichun Liu, Jianhua Li, Yue Xiang, Shuai Hu, Optimal sizing of hydro-PV-pumped storage integrated generation system considering uncertainty of PV, load and price, Energies 12 (15) (2019).
[18] Ahmed Elnozahy, H.S. Ramadan, Farag K. Abo-Elyousr, Efficient metaheuristic Utopia-based multi-objective solutions of optimal battery-mix storage for microgrids, J. Clean. Prod. 303 (2021) 127038.
[19] Omar H. Abdalla, Life SMIEEE, Maged A. Abu Adma, Abdelmonem S. Ahmed, Two-stage robust generation expansion planning considering long- and short-term uncertainties of high share wind energy, Electr. Power Syst. Res. 189 (2020) 106618.
[20] Oluwamayowa O. Amusat, Paul R. Shearing, Eric S. Fraga, Optimal design of hybrid energy systems incorporating stochastic renewable resources fluctuations, J. Energy Storage 15 (2018) 379–399.
[21] Ayşe Selin Kocaman, Pompaj depolamalıhibrid enerji sistemi optimizasyonu-Türkiye için vaka analizi, in: Gazi Üniversitesi Mühendislik Mimarlık Fakültesi Dergisi, Vol. 34, Gazi Üniversitesi, 2019, pp. 53–68, (1).
[22] Ayse Selin Kocaman, Carlos Abad, Tara J Troy, Woonghee Tim Huh, Vijay Modi, A stochastic model for a macroscale hybrid renewable energy system, Renew. Sustain. Energy Rev. 54 (2016) 688–703.
[23] Ayse Selin Kocaman, Emin Ozyoruk, Shantanu Taneja, Vijay Modi, A stochastic framework to evaluate the impact of agricultural load flexibility on the sizing of renewable energy systems, Renew. Energy 152 (2020) 1067–1078.
[24] Özlem Çavuş, Ayşe Selin Kocaman, Özlem Yılmaz, A risk-averse approach for the planning of a hybrid energy system with conventional hydropower, Comput. Oper. Res. 126 (2021).
[25] Homer energy, URL https://www.homerenergy.com/.
[26] Onur Altıntaş, Büşra Ökten, Özlem Karsu, Ayşe Selin Kocaman, Bi-objective optimization of a grid-connected decentralized energy system, Int. J. Energy Res. 42 (2017).
[27] Enercon E-44, URL https://en.wind-turbine-models.com/turbines/531-enercon-e-44.
[28] John R. Birge, François Louveaux, Introduction To Stochastic Programming, Springer-Verlag, New York, NY, USA, 1997.